EVALUATION OF THE EFFECT OF MIXER SETTLER BAFFLES ON LIQUID-LIQUID EXTRACTION VIA CFD SIMULATION

Mohsen OSTAD SHABANI[1], Ali MAZAHERY[2]

Mixer-settlers typically contain an impeller mounted on a shaft, and optionally it can contain baffles. In this study, the effect of the number of baffles on the separation characteristics of the system, and the effect of blade width and inlet velocity on baffles number have been investigated. Computational Fluid Dynamics (CFD) model is developed to predict the separation characteristics. The model has been validated with the help of experimental data for different velocity outlet used in the work. This work has enabled developing efficiency that can produce higher condition than those reported in the previous literature.

Keywords: CFD, separation, baffles

1. Introduction

The importance of separation of immiscible liquid-liquid systems is well known in many industrial fields, such as wastewater treatment and crude oil industry. Study of turbulent flow and computation of its properties in a mixer-settler is a considerable challenge for existing turbulence models. Factors contributing to this difficulty include the non-isotropic nature of flow in a mixer-settler, the complex geometry of rotating impellers and the large disparity in geometric scales present. Existence of baffles also increases the complexity of the flow field. Therefore, it is of great interest to scientists and engineers alike to gain a better understanding of how these various obstructions may influence the fluid and mass transport in channels. Analysis of the turbulent flow pattern and its properties in mixer-settler may be a beneficial tool for equipment design, process scale-up, energy conservation and product quality control [1-3].

Equipments like mixer-settler batteries are commonly used for liquid-liquid extraction and mass transfer processes. Due to the high complexity and cost of the direct experimentation using such equipments, computer simulation becomes very attractive. Algorithms for fast and reliable simulation of single stirred vessels and extraction columns have already been published by some of the present authors, both for steady-state and dynamic conditions. In general,

[1] Materials and Energy Research Center (MERC), Tehran, Iran, e-mail: vahid_ostadshabany@yahoo.com
[2] Materials and Energy Research Center (MERC), Tehran, Iran

knowledge about the settler behavior is scarcer than knowledge about mixers and extraction columns behavior, both in steady and transient states. Existing models for the settler apply only to specific physical equipments at laboratory scale. More recently, an approach based on the population balance equation has been presented [4-7].

In this study, an algorithm able to simulate transient states in a stirred vessel and gravity settler system is described. Providing an adequate combination of mixing and dispersion for the desired degree of extraction is the main function of the mixer. When the impeller rotates, a low pressure region is developed in the vicinity of the impeller. This low pressure region causes mixing of the phases into the mixer [8-11].

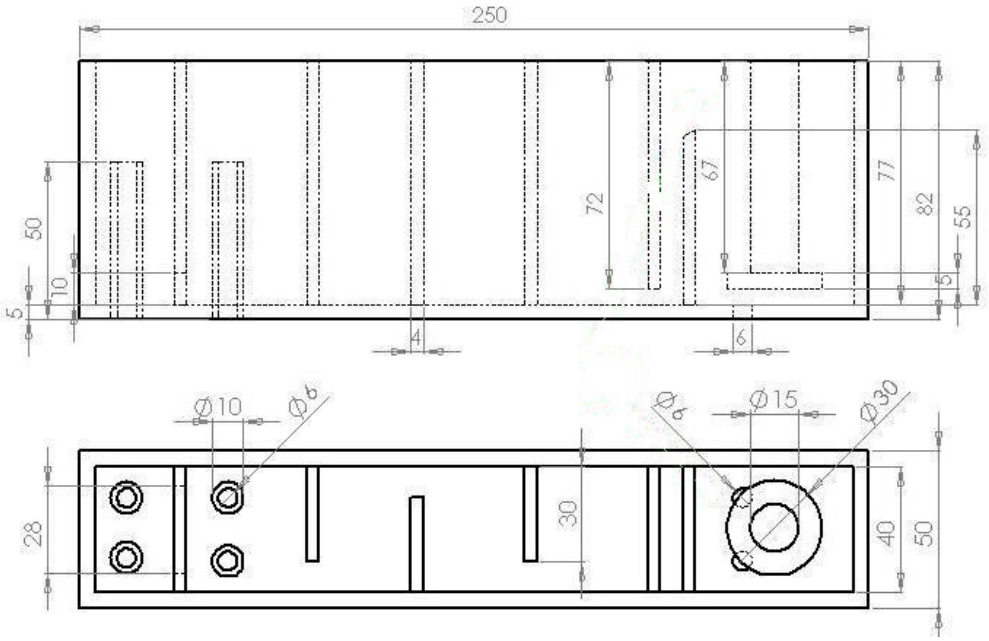

Fig. 1. A side view and top view of the mixer-settler

2. Experimental

Figure 1 shows a side view and top view of the mixer-settler that has been constructed from plexyglass for laboratory experimental purpose. Two inlets are located down of the impeller. The impeller axis was centrally located in the mixer-settler 10 mm from the inlets and mixer bottom. The vertical position of the impeller could be altered, by changing the impeller shafts. The mixer is equipped with four baffles that generated dispersion. The speed could be varied between 0 and 300 rpm by means of a motor controller. The liquid is pumped into the feed

tanks at a known inlet velocity. The aqueous and organic densities (g/cm^3) were 1.06 and 0.79, respectively.

3. CFD

CFD modeling of mechanically agitated baffled tanks poses a unique problem of modeling of interaction between static baffles and rotating impeller. Over the years dedicated efforts have been made to overcome this problem, as a result of which different techniques have evolved and have been validated. Fluid flow field has been calculated by solving the continuity and Navier-Stokes equations along with the standard k-ε turbulence model. The turbulence model included buoyancy, drag, lift and turbulent dispersion forces.
Continuity:

$$\nabla.\rho\vec{\upsilon} = 0 \tag{1}$$

where ρ, is the density and $\vec{\upsilon}$ is the velocity vector.
Momentum balance:

$$\nabla.\rho\vec{\upsilon}\vec{\upsilon} = -\nabla P + (\nabla.\vec{\vec{\tau}}) + \rho g + \vec{F} \tag{2}$$

where $\vec{\vec{\tau}}$ is the stress tensor expressed as:

$$\vec{\vec{\tau}} = \mu[((\nabla\vec{\upsilon}+) + (\nabla\vec{\upsilon}+)T) - \frac{2}{3}\nabla.\vec{\upsilon}] \tag{3}$$

and g, P, μ and $\vec{F}$ are the gravitational force, pressure, dynamic viscosity and external force respectively [1, 11].

3.1. Turbulent model

CFD simulations of the turbulent flow field were carried out using the standard k-ε turbulence model. Two additional transport equations which account for the kinetic energy of turbulence (k), and the rate of dissipation of turbulence (ε), must be solved in order to compute the Reynolds stresses [1, 12, 13]. The hypothesis also introduces another term involving a new variable, k, and the kinetic energy of turbulence. This quantity is defined in terms of the velocity fluctuations u, v, and w in each of the three coordinate directions:

$$k = \frac{1}{2}(\overline{u}^2 + \overline{v}^2 + \overline{w}^2) \tag{4}$$

$$\frac{\delta(\rho k)}{\delta t}+\frac{\delta}{\delta x_i}(\rho U_i k)=\frac{\delta}{\delta x_i}(\mu+\frac{\mu_t}{\sigma_k})\frac{\delta k}{\delta x_i}+G_k-\rho\varepsilon \tag{5}$$

$$\frac{\delta(\rho\varepsilon)}{\delta t}+\frac{\delta}{\delta x_i}(\rho U_i \varepsilon)=\frac{\delta}{\delta x_i}(\mu+\frac{\mu_t}{\sigma_\varepsilon})\frac{\delta \varepsilon}{\delta x_i}+C_1\frac{\varepsilon}{k}G_k+C_2\rho\frac{\varepsilon^2}{k} \tag{6}$$

C_1, C_2, σ_k and σ_ε are considered to be 1.44, 1.92, 1.00 and 1.30, respectively. G_k is a generation term for turbulence which contains products of velocity gradients, and also depends on the turbulent viscosity where ρ is the fluid density, U is the mean velocity vector and μ is the molecular or dynamic viscosity of the fluid. The new constant, μ_t, is the turbulent, or eddy viscosity [1, 11].

$$G_k=\mu_t(\frac{\delta U_i}{\delta x_j}+\frac{\delta U_j}{\delta x_i})\frac{\delta U_j}{\delta x_i} \tag{7}$$

$$\mu_t=\rho C_\mu\frac{k^2}{\varepsilon} \tag{8}$$

3.2. Geometry and the mesh type

The geometry of the mixer settler was modeled in GAMBIT. The flow in the complex channel which is studied in this paper is inherently three-dimensional. A 2D simulation cannot pick up the fluid flows in the third direction and this can result in a lower accuracy of the numerical predictions. In 3D simulations, the baffles, impellers, and other internals can be modeled using their exact geometry. Therefore, in this paper a full 3D flow simulation has been employed. Although Fluent is basically able to treat structural mesh type, the numerical solver of it did not reach any convergence. Therefore, a completely unstructured grid was generated which was optimized for its performance with approximately 0.5, 0.6, 0.7, 0.8, 0.9, 1 million cells. This nodalization includes every flow-relevant detail and abstains from simplifications. Furthermore, hexahedral cells have been applied for meshing model [1].

3.3. Boundary conditions and solver

A velocity magnitude is set at the inlet and zero gauge pressure is set at the outlet. No velocity slip exists at solid walls and the standard wall functions are used for near-wall treatment. At the inlet, a constant flow rate was specified and at the outflow of the mixing channel, pressure outlet boundary condition was assumed. The momentum reflection back into the computational domain was

assumed to be normal to the outlet. Turbulence of the fluid back into the computational domain was specified approximately by the turbulent intensity and hydraulic diameter of the flow channel.

Fluid motion is calculated by directly solving the Navier-Stokes equations. Second order discretization scheme is used for momentum, turbulent kinetic energy and for the energy dissipation. Commercial CFD software, Fluent 6.3 was used to simulate the flow fields under different operating conditions. SIMPLE (Semi-Implicit Method to solve Pressure Linked Equations) method was used for the pressure-velocity coupling. SIMPLE determines the pressure field indirectly by closing the discretised momentum equations with the continuity equations in a sequential manner. A 3D, segregated, implicit, steady solver algorithm was used for predicting the velocity and turbulence fields. Then k– ε turbulence model was defined. Under relaxation factors, 0.3, 1.0, 1.0, 0.7, 0.8, and 0.8 were chosen for pressure, density, body forces, momentum, kinetic energy, and dissipation, respectively. During the solution for mixing, solutions for the flow field were held constant [1, 13-15].

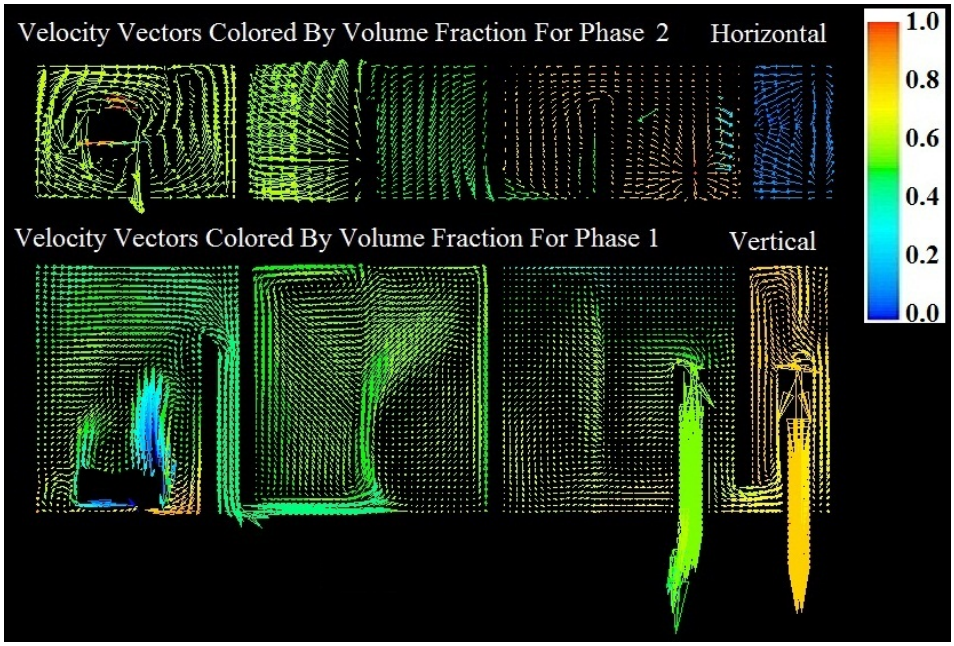

Fig. 2. Velocity vectors colored by volume fraction with 4 baffles, inlet velocity 0.5 (m/s) and blade width 7(mm)

The method to judge convergence was to monitor the magnitude of scaled residuals. Residuals are defined as the imbalance in each conservation equation following each iteration. The convergence criteria was set that the governing

equations are iteratively solved until at all nodes in the computational domain the relative changes in pressure and velocity components between two successive iterations become less than 10^{-6} (residual monitors).

4. Results

Fig. 2 shows the velocity vectors colored by volume fraction with 4 baffles, inlet velocity 0.5 (m/s) and blade width 7 (mm) and figure 3 shows path lines colored by volume fraction with 4 baffles, inlet velocity 0.3 (m/s) and blade width 4 (mm). In the mixing process of the primary and secondary fluid, the momentum of the two fluids is exchanged through the flow layer. The function of the mixer is to provide an adequate combination of mixing and dispersion for the desired degree of extraction. Mixers are square in cross section and are fitted with a full width vertical baffle to prevent vortex formation. The functions of baffles are to ensure even distribution and to reduce settler turbulence. Reduction of the settler size is required to achieve the phase separation. Increased size leads to higher capital cost for equipment, increased plant area, and higher organic inventory. Nevertheless, settler design procedures have frequently proven to be unreliable, resulting in the use of large safety factors, and consequent settler overdesign.

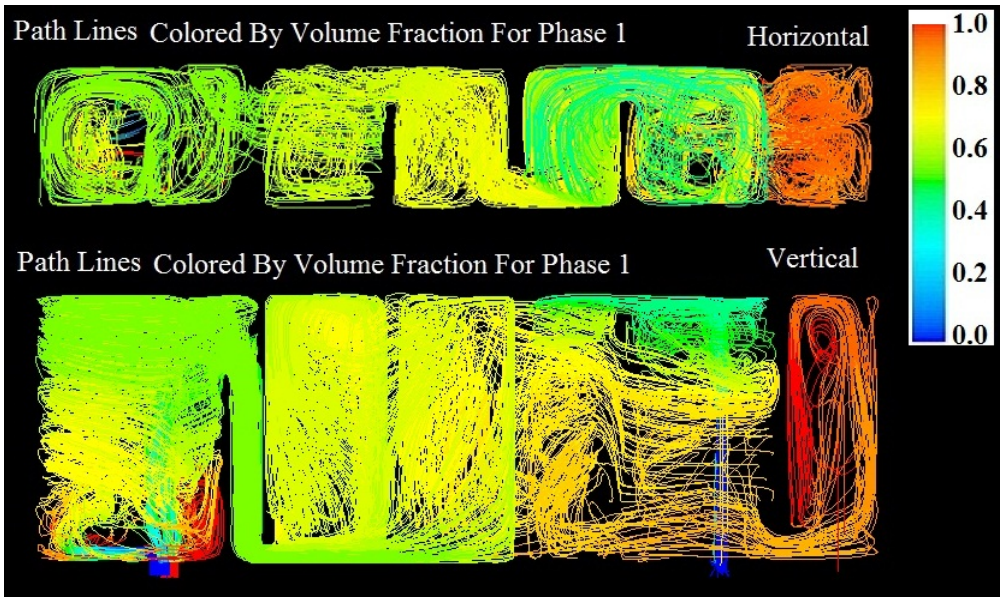

Fig. 3. Path lines colored by volume fraction with 4 baffles, inlet velocity 0.3 (m/s) and blade width 4 (mm)

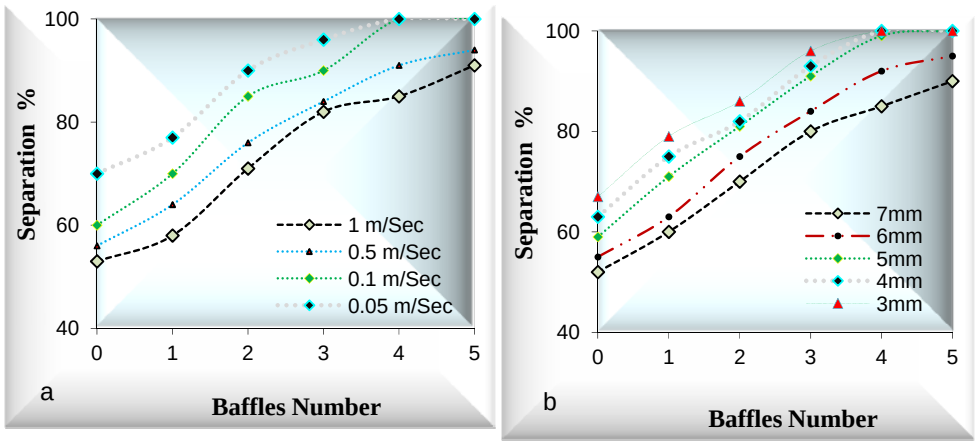

Fig. 4. Amount of separation percentage of organic phase as a function of baffles number for impeller speed 100 (rpm) in organic outlet, a: for blade width 5 (mm) in different inlet velocity and b: for inlet velocity 0.1 (m/s) in different blade width

Fig. 4a shows the amount of separation percentage of organic phase as a function of baffles number in organic outlet for impeller speed 100 (rpm) and blade width 5 mm in different inlet velocity. The amount of separation increases with increasing baffles number, according to CFD data. This is obvious, because when baffles number increased, path increased and condition for separation improved. When the velocity inlet is increased, greater mixing could be obtained in constant impeller speed. However, when inlet velocity is more than 0.1 (m/s) with 4 baffles, there is not enough time for separation of the phases. In other word, increased mixing intensity can produce a dispersion which is more difficult to separate, resulting in greater settler size and more use of baffles. Fig. 4b shows the amount of separation percentage of organic phase as a function of baffles number in organic outlet for impeller speed 100 (rpm) and inlet velocity 0.1 (m/s) in different blade width. According to previous work [16], mixing increases with increasing blade width. When the blade width (contact area) increases, it induces an increase in the velocity of the mixer and an improvement in the mixing condition. But when blade width is more than 5 (mm) with 4 baffles there is not enough time for separation phases; increased mixing intensity results in increasing consume power.

Fig. 5a shows the contour of volume fraction for phases, with 2 baffles, inlet velocity 0.5 (m/s) and blade width 4 mm in mixer-settler, obtained by CFD and fig. 5b shows the contour of volume fraction for phases, with 4 baffles, inlet velocity 0.2 (m/s) and blade width 7 mm. According to figure 5a, there is not enough time for separation phases and a dispersion which is more difficult to

separate, can be produced resulting in more baffles numbers or decrease blade width or inlet velocity.

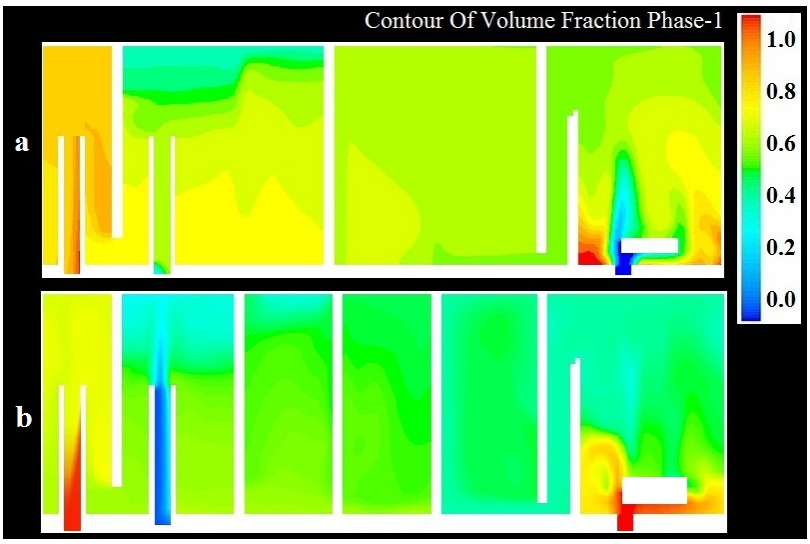

Fig. 5. Contour of volume fraction for phases, a: with 2 baffles, inlet velocity 0.5 (m/s) and blade width 4 mm and b: with 4 baffles, inlet velocity 0.2 (m/s) and blade width 7 (mm)

5. Validation of CFD simulations

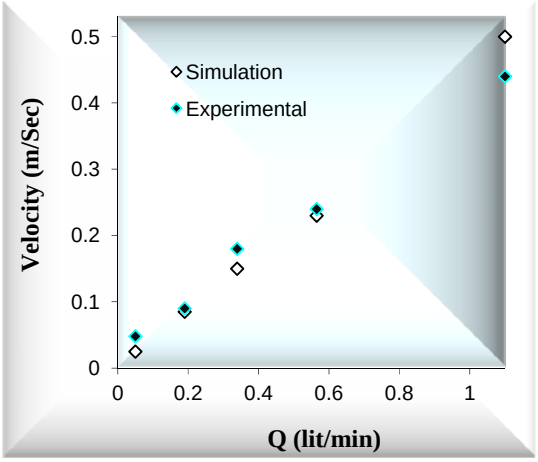

Fig. 6. Outlet velocity as a function of total flow rate with 4 baffles and blade width 5 (mm)

The outlet velocities obtained by simulation and experimental are compared in this research. The outlet velocity as a function of total flow rate with 4 baffles and blade width 5 mm is shown in figure 6. Validation is a necessary

part of the modelling process by quantifying level of agreement that can be attained between numerical predictions and experiments. High consistency of outlet velocity in experimental and simulation is noted, according to the results.

6. Conclusion

In this study, the influences of the number of mixer settler baffles, blade width and inlet velocity in separation have been investigated. The CFD model predictions are compared with the experimental data. The insertion of the appropriate number of baffles clearly improves the extent of liquid separation. However, the excessive baffling, inlet velocity and blade width would interrupt the liquid mixing and increase the mixing time. Clearly, the operation of mixer-settler is required to be optimized. In this research, the operation of mixer-settler was optimized using 4 baffles when inlet velocity and blade width were 0.1 (m/s) and 5 (mm), respectively.

R E F E R E N C E S

[1]. *E. F. Gomes, M. M. L. Guimarães, L. M. Ribeiro*, Numerical modelling of a gravity settler in dynamic conditions, Advances in Engineering Software, 38, 2007, pp. 810-817.

[2]. *M. H. Vakili, M. Esfahany*, CFD analysis of turbulence in a baffled stirred tank, a three-compartment model, Chemical Engineering Science, 64, 2009, pp. 351-362.

[3]. *K. Takahashi, A. Abdel, S. A. Tawab, T. Yajima, F. Kawaizumi*, Extraction of rare earth metals with a multistage mixer-settler extraction column, Chemical Engineering Science, 57, 2002, pp. 469-478.

[4]. *Y. N. Chiu, J. Naser, K. F. Ngian, K. C. Pratt*, Numerical simulations of the reactive mixing in a commercially operated stirred ethoxylation reactor, Chemical Engineering Science, 63(11), 2008, pp. 3008-3023.

[5]. *H. D. Zughbi, M. A. Rakib*, Mixing in a fluid jet agitated tank: efects of jet angle and elevation and number of jets, Chemical Engineering Science, 59, 2004, pp. 829-842.

[6]. *R. N. Reeve, J. C. Godfry*, Phase inversion during liquid-liquid mixing in continues flow, pump-mix, agitated tanks, Institution of Chemical Engineers, Trans IChemE, vol 80, part A, November 2002.

[7]. *M. T.Mostaedi, J. Safdari*, *M. A. Moosavian*, *M. G. Maragheh*, Flooding characteristics in a Hanson mixer settler extraction column, Chemical Engineering and Processing, 48, 2009, pp. 1249-1254.

[8]. *K. Pianthong, W. Seehanam*, *M. Behnia*, *T. Sriveerakul*, Investigation and improvement of ejector refrigeration system using computational fluid dynamics technique, Energy Conversion and Management, 48(9), 2007, pp. 2556-2564.

[9]. *R. N. Meroney, P. E. Colorado*, CFD simulation of mechanical draft tube mixing in anaerobic digester tanks, Water Research, 43, 2009 , pp. 1040-1050.

[10]. *C. Srilatha, T. P. Mundada, A. W. Patwardhan*, Scale-up of pump-mix mixers using CFD, Chemical Engineering Research and Design, 88, 2010, pp. 10–22.

[11]. *Binxin Wu*, CFD simulation of mixing in egg-shaped anaerobic digesters, Water Research, 2009, pp. 1-13.

[12]. *B. N. Murthy, J. B. Joshi*, Assessment of standard k–ε, RSM and LES turbulence models in a baffled stirred vessel agitated by various impeller designs, Chemical Engineering Science, 63, 2008, pp. 5468-5495.
[13]. *K. K. Singh, K. T. Shenoy*, *A. K. Mahendra*, *S. K. Ghosh*, Artificial neural network based modelling of head and power characteristics of pump-mixer, Chemical Engineering Science, 59, 2004, pp. 2937-2945.
[14]. *L. Eckert*, Aspects of phase separation in experimental mixer-settler using two solvent extraction system, B. A. Sc, The University of British Columbia, 1984.
[15]. *K. K. Singh, S. M. Mahajani*, *K. T. Shenoy*, *A. W. Patwardhan*, *S. K. Ghosh*, CFD modeling of pilot-scale pump-mixer: Single-phase head and power characteristics, Chemical Engineering Science, 62, 2007, pp. 1308-1322.
[16]. *M. O. Shabani*, *M. Alizadeh*, *A. Mazahery*, Fluid flow characterization of liquid-liquid mixing in mixer-settler, Engineering with Computers, 27, 2011, pp. 373-379.